THE ASTROPHYSICAL JOURNAL, 361:49–62, 1990 September 20

A REDSHIFT SURVEY OF *IRAS* GALAXIES. I. SAMPLE SELECTION[1]

MICHAEL A. STRAUSS[2,3] AND MARC DAVIS
Astronomy and Physics Departments, University of California, Berkeley
AMOS YAHIL
Astronomy Program, State University of New York at Stony Brook
AND
JOHN P. HUCHRA
Center for Astrophysics
Received 1990 January 20; accepted 1990 March 20

ABSTRACT

We have extracted a complete all-sky sample of objects, flux-limited at 60 μm from the data base of the *Infrared Astronomical Satellite* (*IRAS*). The sample consists of 5014 objects, of which 2649 are galaxies and 13 are not yet identified. The sample covers 87.6% of the sky. This is the first paper in a series describing a redshift survey based on this sample, which we use to study the nature of the large-scale distribution of galaxies in the nearby universe. In order to study large-scale structure with this sample, it must be free of systematic biases, and we present our selection procedure in detail. We apply corrections for a major systematic effect in the flux densities listed in the *IRAS Point Source Catalog*: sources resolved by the *IRAS* beam have flux densities systematically underestimated. In addition, accurate flux densities are obtained for sources flagged as variable, or of moderate flux quality at 60 μm. The *IRAS* detectors suffered radiation-induced responsivity enhancement (hysteresis) due to crossings of the satellite scans across the Galactic plane; this effect is measured and is shown to be negligible.

Subject headings: galaxies: redshifts — infrared: sources

I. INTRODUCTION

In any branch of astronomy involving statistical results drawn from large surveys of objects, it is imperative to use samples whose selection procedure is well defined and as free as possible from systematic biases and effects. This ideal is of course rarely achieved in practice. The need for unbiased samples is nowhere more acute than in large-scale surveys of galaxies, where controversies have raged over the reality of certain subtle effects: do they have physical significance, or are they mimicked by observer selection (cf. the series of opposing papers by Geller, de Lapparent, and Kurtz 1984 and de Lapparent, Kurtz, and Geller 1986 vs. Groth and Peebles 1986*a*, *b* and Brown and Groth 1989 over the reality of the 2°.5 break observed in the angular galaxy correlation function derived from the Shane-Wirtanen 1967 counts, or Bahcall and Soneira 1983 vs. Sutherland 1988 and Dekel *et al.* 1989 over the significance of the Abell cluster correlation function).

We have completed a redshift survey of galaxies detected by the *Infrared Astronomical Satellite*[4] (*IRAS*) and have labored to free our sample of all known systematic effects due to instrumental and observational biases. As discussed in detail in the following papers in this series, the almost full sky coverage of the *IRAS* survey, the well-calibrated flux densities, and the lack of Galactic extinction in the far-infrared, allow analyses of such quantities as the spatial dipole moment of the sample and the velocity field due to the density distribution within the volume in which the nearest few superclusters lie. In this paper, we discuss in detail our sample selection and correction for systematic effects. Our aim is to obtain a complete sample of galaxies, uniformly selected over most of the sky and flux-limited at 60 μm, from which we can draw conclusions about the nature of the large-scale galaxy distribution with confidence that there are little systematic calibration errors left which are dependent on position or redshift.

The sample is drawn largely from the *IRAS Point Source Catalog*, Version 2 (1988; hereafter PSC); in § II, we discuss and rationalize our selection procedures. The most important bias in the PSC is the fact that sources resolved by the *IRAS* beam in any given passband have flux densities that are underestimated; our corrections for this effect are discussed in detail in § III. In addition, accurate flux densities are obtained for objects flagged as variable, and of moderate flux quality at 60 μm. In § IV, we measure the effect of hysteresis caused by radiation-induced responsivity enhancement of the *IRAS* detectors as the telescope scanned across the Galactic plane; we show that this effect is smaller than 1% over most of the sky. Discussion and summary are presented in § V. Future papers in this series will present the results of our optical observations of the sample and discuss the large-scale distribution of *IRAS* galaxies and the inferred velocity field.

II. THE SELECTION CRITERIA FOR THE SAMPLE

a) Philosophy and Background

In order to understand the nature of the *IRAS* data base, it is necessary to be familiar with the basic workings of the *IRAS*

[1] Based in part on data obtained at Lick Observatory, operated by the University of California; the Multiple Mirror Telescope, a joint facility of the Smithsonian Astrophysical Observatory and the University of Arizona; and Cerro Tololo Inter-American Observatory, operated by the Association of Universities for Research in Astronomy, Inc., under contract with the National Science Foundation.

[2] Also Astronomy Department, California Institute of Technology.

[3] Norris Fellow.

[4] The *Infrared Astronomical Satellite* was developed and operated by the US National Aeronautics and Space Administration (NASA), the Netherlands Agency for Aerospace Programs (NIVR), and the UK Science and Engineering Research Council (SERC).

satellite and the strategy of the all-sky survey. A thorough account can be found in Neugebauer *et al.* (1984), and in the *IRAS Explanatory Supplement* (1988, hereafter ES). *IRAS* consisted of an f/9.6 57 cm Ritchey-Chrétien mirror mounted inside a superfluid helium dewar. The satellite flew between 1983 January and November, and surveyed 96% of the sky in four broad photometric bands, roughly centered on 12, 25, 60, and 100 μm, respectively (ES, Figure II.C.9.*b*). The survey was done by continuously scanning along lines of constant ecliptic longitude at a rate of $3'.85\ s^{-1}$. The focal plane (§ II.C.4 of ES) consisted of 62 infrared detectors, with rectangular slits oriented with the long dimension in the cross-scan direction; thus, the raw *IRAS* data consist of flux from each detector as a function of time. A zero-sum filter of central width 2′ at 60 μm, pictured in ES Figure V.C.1.*a*, was run over the individual scans. The local noise was calculated simultaneously. Any source with a signal-to-noise ratio greater than 3.7 was convolved with a template of the response of the detector to a point source; sources with correlation coefficients (ES § V.C.4) greater than or equal to 0.87 were retained. The reality of the source was checked by asking for consistency between detections in different channels in a given scan (seconds confirmation) and between adjacent overlapping scans (hours confirmation); confirmed sources were then entered into the Working Survey Data Base, after using the response curve of the *IRAS* detectors to convert flux densities into fluxes. Finally, individual detections from the Working Survey Data Base were collected together, and the individual hours-confirmed flux densities for each source were log-averaged with weights proportional to the inverse square of their log errors, to obtain the final PSC flux density. A source with two or more separate hours-confirmed detections is called "weeks-confirmed." At 60 μm, most sources have listed positions good to $\approx 15''$ (1 σ errors) (ES § VII.C.1.*a*), and the flux densities have quoted errors of $\sim 10\%$.

We wish to extract from the *IRAS* data base a flux-limited sample of galaxies with flux densities as accurate as possible, with complete sky coverage and a uniform flux density limit. We will be especially concerned with selection biases that depend on position on the sky or on the distance of the object in question because such effects can easily mask or mimic features in the large-scale distribution of galaxies. The first issue is the nature of a criterion to select galaxies from the PSC. The PSC consists of 245,889 objects, of which it is thought that approximately 20,000 are galaxies (Soifer, Houck, and Neugebauer 1987); the remainder are mostly stars, H II regions, and clumps of infrared "cirrus." Galaxies can be distinguished from stars by their characteristic colors (e.g., Walker *et al.* 1989). While infrared-bright stars have spectral energy distributions in the infrared that peak in the 12 μm band, typically due to circumstellar dust shells heated to temperatures greater than 100 K (Cohen *et al.* 1987), normal galaxies are quite a bit cooler, peaking at 60 μm (Heisler and Vader 1989) or 100 μm. Only the most active galaxies are stronger at 25 than at 60 μm (e.g., Low *et al.* 1988). The *IRAS* emission from galaxies is modeled to arise from a combination of three sources (Helou 1986; Crawford and Rowan-Robinson 1986; Bothun, Lonsdale, and Rice 1989): interstellar dust heated by the general interstellar radiation field, which dominates 60 μm emission in galaxies like the Milky Way and M31; interstellar dust directly associated with, and heated by, active centers of star formation, which dominates in active star-forming galaxies, nearby extreme examples of which are M82 and NGC 253, and finally, emission from an active nucleus, which dominates the far-infrared spectral energy distribution in galaxies like 3C 273. By definition, of course, the first two emission mechanisms listed are exactly what account for the *IRAS* emission from infrared "cirrus" (Low *et al.* 1984; Puget 1988) and H II regions (Hughes and MacLeod 1989), respectively, and any criterion that selects galaxies will of necessity also select large numbers of these objects in our own Galaxy at low Galactic latitudes.

Galaxy catalogs have been selected from the PSC by a variety of groups. Perhaps the most straightforward criterion is that of the *Cataloged Galaxies in the IRAS Survey*, Version 2 (1989, hereafter CGIRAS) which is a sample of 11,444 known galaxies created by matching the PSC against a variety of optically selected galaxy catalogs. However, we wish our selection procedure to be based purely on infrared criteria and therefore reject this approach. Another simple criterion is that of Soifer *et al.* (1987), who created a flux-limited sample of galaxies by simply looking at *all* 60 μm sources of high flux quality brighter than 5.4 Jy at high Galactic latitudes. This procedure does work well in regions of the sky where contamination from Galactic sources is likely to be small but would become quite useless at low Galactic latitudes. All other workers have selected galaxies based on a color criterion, in which they have taken advantage of the fact that the spectral energy distributions of galaxies in the *IRAS* passbands peak at 60 or 100 μm (see the thorough discussion of the colors of *IRAS* sources in Walker *et al.* 1989). Meiksin and Davis (1986, hereafter MD) used the color criterion $f_{60}/f_{12} > 3$, where f_λ is the flux per unit frequency (flux density) of an object at wavelength λ in janskys. Yahil, Walker, and Rowan-Robinson (1986, hereafter YWR) used the somewhat less restrictive color criterion $f_{60}/f_{25} > \frac{1}{3}$, while other groups (e.g., Meurs and Harmon 1988; Rowan-Robinson 1988; Lu *et al.* 1990; Babul and Postman 1990) have used more complicated criteria involving *IRAS* colors and other *IRAS* information in order to decrease the contamination from cirrus and stars.

b) Our Criteria

For the present survey, we wish to maximize the number of galaxies included. Because we obtain optical identifications for *every* object in our sample, we can afford to have some degree of contamination from Galactic objects. Our criteria have changed somewhat since we started this program, and it is worthwhile to describe their evolution.

Originally, we adopted a set of criteria based on those of MD; that is, we selected objects from the PSC with $f_{60}/f_{12} > 3$, using PSC listed fluxes or upper limits. Our flux limit is 1.936 Jy, that of the brightest quartile of the sample of MD. We can test the efficacy of the MD color criterion in selecting galaxies as follows: 32 of the 2014 galaxies in the CGIRAS with $f_{60} >$ 1.936 Jy have $f_{60}/f_{12} < 3$; $\sim 81\%$ of these have only quoted upper limits for the flux density at 12 μm. Thus the efficacy of the MD criterion is better than 98%. Note that MD quote a somewhat lower efficacy of 73%. This is probably due to contamination of their statistics by objects with f_{60} less than 0.75 Jy; because objects in the PSC with undetected 12 μm emission are listed with a flux density of 0.25 Jy or larger, no objects with $f_{60} < 0.75$ Jy can satisfy the color criterion.

However, as pointed out by Dey, Strauss, and Huchra (1990), there is a strong correlation between the f_{60}/f_{12} color and the 60 μm flux density, in the sense that fainter objects tend to have a larger 12 μm flux density relative to their 60 μm emission. Figure 1 shows a color-magnitude diagram of all

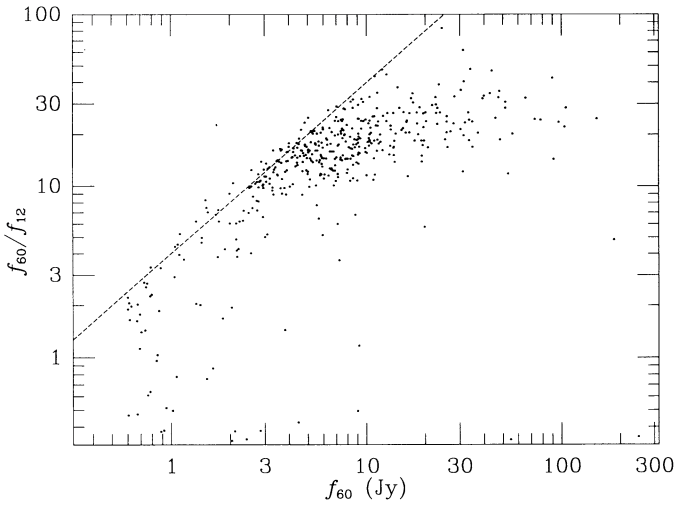

FIG. 1.—Plot of f_{60}/f_{12} as a function of f_{60} for objects in the PSC with $|b| > 30°$, detections at 12 μm, and outside the Magellanic Clouds. PSC fluxes are used here and the following plots, uncorrected by ADDSCANs. Notice the strong dependence of the color on flux density.

objects in the PSC above 1.2 Jy, with detections at 12 and 60 μm, Galactic latitude $|b| > 30°$, and more than 3° and 6° from the Small and Large Magellanic Clouds, respectively. See also the similar plot in Figure III.B.4 of the *Explanatory Supplement to the IRAS Faint Source Survey* (Moshir *et al.* 1989). At faint levels in the PSC, the quoted flux densities have a large intrinsic scatter (ES, Fig. XII.A.5). Thus a source with a true flux density at 12 μm fainter than 0.25 Jy has an appreciable probability of being scattered by measurement errors to larger flux density, thus artificially decreasing the f_{60}/f_{12} color. In fact, we have obtained more accurate flux densities for many of these objects using the ADDSCAN procedure (§ III*a* below) and find that the PSC 12 μm flux densities are often overestimated by a factor of 5!

Moreover, because *IRAS* covered the sky to different depths in different areas of the sky, the noise levels are *not* uniform with respect to position, which means that the MD color criterion rejects galaxies preferentially in certain regions of the sky. Figure 2 shows the distribution on the sky of objects in the CGIRAS with $f_{60}/f_{12} < 3$ and $f_{60} > 1.2$ Jy[5]; above the Galactic plane, these objects simply trace the regions of the sky that *IRAS* covered with two hour-confirming scans rather than three (cf. ES Fig. I.C.1).

Although this becomes a serious problem only at flux densities fainter than 1.936 Jy at 60 μm, we have decided to use a more lenient color criterion for the present sample to remove any possible source of bias. Figure 3 shows a color-color diagram for the 3566 objects in the CGIRAS with detections at 60 μm above 1.2 Jy. Quoted upper limits were used for sources undetected at 12 or 25 μm. Objects above the horizontal dashed line satisfy the MD color criterion ($f_{60}/f_{12} > 3$), while objects to the right of the vertical dashed line satisfy that of YWR ($f_{60}/f_{25} > \frac{1}{3}$). Our new color criterion is represented by the diagonal dashed line ($f_{60}^2 > f_{12} f_{25}$). There are only 38 objects in the CGIRAS above 0.6 Jy, the completeness limit of the PSC at 60 μm, that do not satisfy this new color criterion, and only 11 above 1.2 Jy. They seem to be distributed uniformly around the sky. See Strauss (1989) for a similar plot made directly from the PSC.

There is another serious bias in our original sample. Like MD, we chose only objects that were of highest flux quality at 60 μm, that is, that had two clean hours-confirmed detections (ES, § V.H.5). Clearly, however, if a region of sky is covered 3 times by *IRAS*, it has a greater chance of being detected twice than if covered 2 times. Figure 4 shows the sky distribution of objects in the PSC with moderate flux quality at 60 μm (i.e., those with a single high-quality hours-confirmed detection at 60 μm), satisfying our color criterion, and with $f_{60} > 0.6$ Jy. Again, the regions of sky covered only twice by the satellite clearly stand out (as do the excluded regions of MD heavily contaminated by Galactic objects). We have therefore included all objects of moderate flux quality at 60 μm in our sample.

Our sample is thus defined by the following criteria:

1. $f_{60}^2 > f_{12} f_{25}$, based on flux densities or upper limits listed in the PSC;

[5] We use 1.2 Jy as the limiting flux in several of these diagnostic plots because this is the flux limit of a deeper survey we have started, selected using the same criteria.

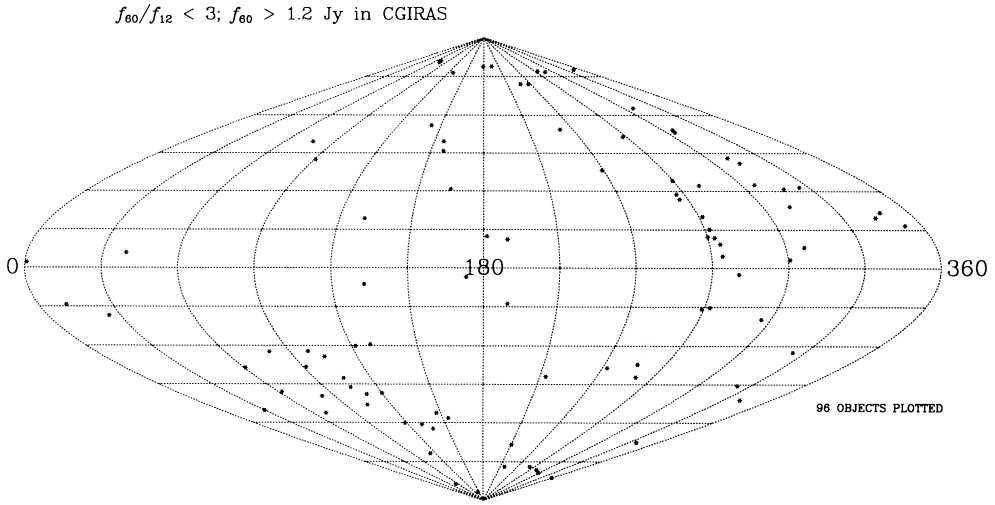

FIG. 2.—The sky distribution of objects in the CGIRAS with $f_{60}/f_{12} < 3$ and $f_{60} > 1.2$ Jy. This is an equal-area projection in Galactic coordinates. Note the strong concentration of objects at positive latitudes with $270° < l < 360°$ and at negative latitudes with $90° < l < 150°$; these are the regions with two hours-confirmed coverages in the *IRAS* survey.

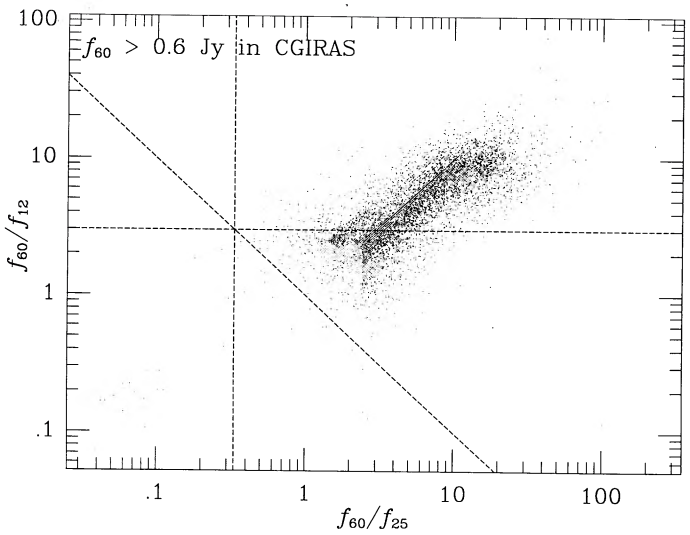

FIG. 3.—Color-color plot, f_{60}/f_{12} vs. f_{60}/f_{25}, for objects in the CGIRAS. The horizontal dashed line is the limit of the MD color criterion ($f_{60}/f_{12} > 3$), the vertical line is that of the YWR color criterion ($f_{60}/f_{25} > \frac{1}{3}$), and the diagonal line is that of the color criterion used for the present study ($f_{60}^2 > f_{12} f_{25}$). The strong diagonal line of sources along $f_{60}/f_{12} = f_{60}/f_{25}$ is due to sources with nondetections at both 12 and 25 μm; they are listed in the PSC with fluxes of 0.25 Jy in both bands.

2. Flux quality at 60 μm equal to 2 or 3 (moderate or high);

3. $f_{60} > 1.936$ Jy, after correcting for the effects discussed below in § III.

The flux density limit was imposed for two reasons: This is a flux density well above the limit below which systematic problems in the *IRAS* flux scale become apparent (B. T. Soifer, private communication), and it defines a sample of the order of 2650 galaxies, meaning that redshifts could be obtained for the entire sample in ~ 2 yr.

Note that unlike MD, variability flags and the nature of the identifications (Meurs and Harmon 1988) were *not* used as selection criteria.

We will take the flux scale defined by the PSC as our ultimate authority in this work. A number of corrections could conceivably be applied to the flux densities (see Fisher *et al.* 1990). First, the PSC passbands are quite broad (see ES, Fig. II.C.9.*b*), and, in order to calculate flux densities, one must assume a spectral shape; in the PSC, a ν^{-1} spectrum was used. In principle, a more accurate flux density can be derived for individual sources using the listed flux densities in the other bands and an iteration procedure (ES § VI.C.3; Saunders *et al.* 1990; Fisher *et al.* 1990). We have chosen *not* to do this for the sake of simplicity, assuming that spectral shape is not in any way correlated with large-scale structure.

There are additional corrections that might be applied due to relativistic effects and the change in the passband due to redshift. Fisher *et al.* (1990) have shown that the mean differential correction between galaxies at low redshift and those at 10,000 km s^{-1}, the maximum redshifts we consider in our large-scale structure analyses, is $\sim 4\%$.

Saunders *et al.* (1990; see also Hacking *et al.* 1987) show that there is evidence for evolution of the *IRAS* source density within redshifts of $z \lesssim 0.2$. Fisher *et al.* (1990) find marginal evidence for such an effect using a V/V_{max} test (Schmidt 1968) on the present sample, but we will ignore this possibility here.

Finally, the 60 μm flux densities have errors log-normally distributed with an effective σ of $\sim 10\%$. This will cause a Malmquist systematic overestimation of the flux densities of order 1.5%. We have not applied any correction for this effect here.

c) *Excluded Regions*

Because MD did not do any follow-up identification to their sample, they restricted themselves to regions of the sky not unduly contaminated by infrared cirrus and other Galactic objects. Thus, they selected by eye a series of "excluded zones" with high source density. In particular, the region $|b| < 10°$ was excluded, as were areas around the Orion-Taurus and Ophiuchus star-forming regions, the Large and Small Magellanic Clouds, and M31 (MD Fig. 3). This left 76% of the sky included in their survey. We started the present survey using the same excluded regions, but later extended the survey into the MD excluded zones, with the following effects in mind. At very low Galactic latitudes, where the source density is changing rapidly, lag in the noise estimator caused all but the brightest sources to be rejected down-scan of the plane, a process

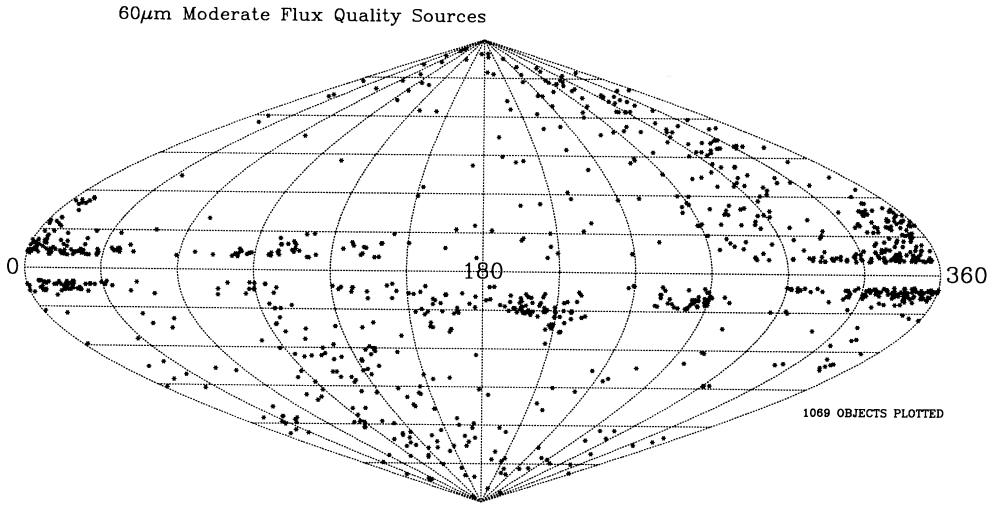

FIG. 4.—The sky distribution of objects of moderate flux quality at 60 μm in the PSC, satisfying our color criterion, with $f_{60} > 0.6$ Jy. Objects falling within the excluded zones of Fig. 5 are not included here. Notice the similarity of this distribution to that in Fig. 2.

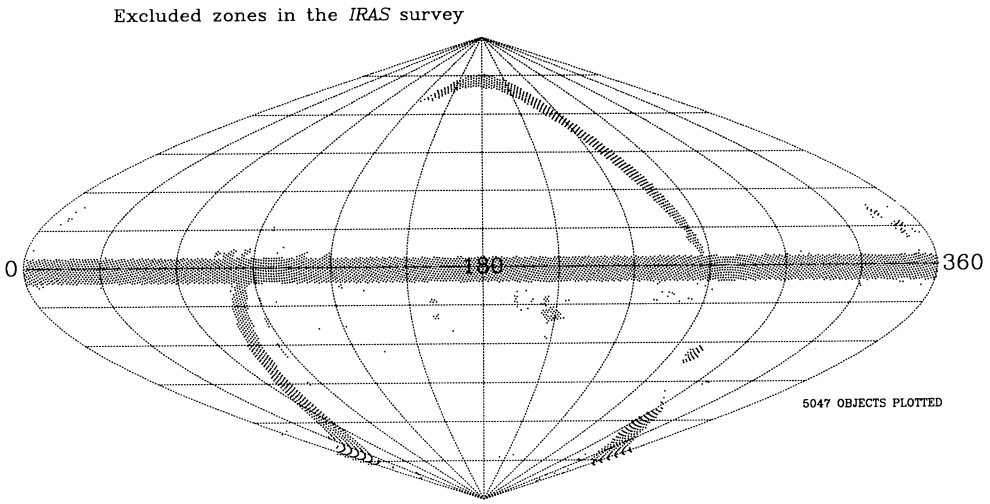

FIG. 5.—The regions of sky not included in the present survey. They include the region $|b| < 5°$, areas affected by confusion at 60 μm, and two strips of constant ecliptic longitude not included in the PSC.

called "shadowing" (ES § VIII.D.6). At no Galactic longitude is this effect important at $|b| > 5°$; thus, we restricted ourselves to Galactic latitudes above 5°.

The *IRAS* beam at 60 μm has a full width at half-maximum of $\sim 1.'5$ (ES, Fig. V.C.2.*c*), which makes confusion an issue in regions of high source density. In the compilation of the PSC, confusion was tested for as follows. The sky was divided into 41,167 approximately square bins of area 1 deg^2, defined by their ecliptic coordinates; if more than 16 60 μm sources were detected in any one bin, all the objects of the bin were processed using a special algorithm. Because we desire a data sample selected as uniformly as possible, we have excluded sources in all such bins. There are 225 such bins at $|b| > 5°$, concentrated in Orion, Ophiuchus, and the Magellanic Clouds. Finally, the *IRAS* mission was not quite completed; there are two regions, each of approximately constant ecliptic longitude and totaling 4% of the sky, that were not covered with two hours-confirming scans (the minimum for entry into the PSC) by the survey when the satellite ran out of liquid helium in 1983 November. Figure 5 shows the sky distribution, in Galactic coordinates, of the regions of sky thus excluded in the present survey; they cover 12.34% of the sky.

We are now ready to define the master catalog from which our sample was extracted. It is outlined in Table 1.

Objects for the present survey satisfying the criteria listed above were selected from the PSC outside the excluded regions shown in Figure 5. We will see below that objects within and outside the original MD excluded zones were treated differently, so we list them separately in Table 1 as the first two rows. This includes all objects with PSC flux densities above 1.936 Jy satisfying the criteria above, for which more accurate fluxes using the ADDSCAN procedure, described below, were not obtained. In addition, objects resolved by the *IRAS* beam at 60 μm, flagged as variable, or of moderate flux quality at 60 μm, may have PSC flux densities underestimated, as detailed in the following section. Thus, we also extracted from the PSC all objects with listed flux densities above 0.6 Jy (the completeness limit of the PSC at 60 μm), which were flagged as variable, extended, or of moderate flux quality at 60 μm. Rows 3 and 4 of Table 1 include all such objects which satisfy the color criterion $f_{60}^2 > f_{12} f_{25}$, *based on PSC listed flux densities.* These objects were included in our final catalog only if more accurate flux densities obtained from the ADDSCAN procedure (§ III*a*) revealed them to be above 1.936 Jy at 60 μm (col. [2]).

Finally, there is a handful of bright objects that were not included in the PSC due to a processing error; they are listed in ES, Table XII.A.5 and included in our catalog (entry 5). Entry 6 will be described below in § III*b*.

For each entry we indicate the total number of objects, the number with final flux density greater than 1.936 Jy, the number of those that are confirmed galaxies, and, finally, the number remaining to be observed. The 13 unobserved objects

TABLE 1

CLASSIFICATION OF OBJECTS IN SAMPLE

Entry	Total	>1.936 Jy	Galaxies	Unobserved	Sample
1	1929	1929	1706	0	Not ADDSCANed; outside excluded zones
2	1039	1039	173	1	Not ADDSCANed; in excluded zones
3	1694	723	618	2	ADDSCANed; outside excluded zones
4	1891	1261	92	10	ADDSCANed; in excluded zones
5	3	3	1	0	Added objects from ES
6	59	13[a]	46[b]	0	Galaxies from LOGC
Totals	6615	5014	2649	13[c]	

[a] Galaxies without PSC counterparts.
[b] Galaxies with PSC counterparts.
[c] Few likely to be galaxies.

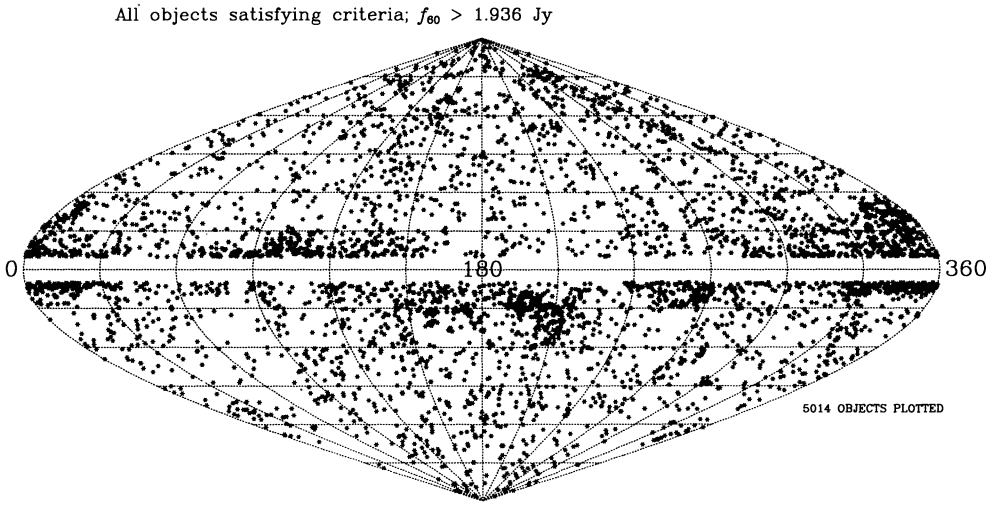

FIG. 6.—The sky distribution of all the sources satisfying our selection criteria.

all seem to be associated with infrared cirrus or other Galactic objects, on the basis of finding charts made from the POSS or ESO plates.

The sky distribution of all the sources above 1.936 Jy included in Table 1 is shown in Galactic coordinates in Figure 6. Notice that the sources are in fact greatly concentrated, toward the Galactic plane, and to the star-forming regions in Orion ($l = 210°$, $b = -20°$) and Ophiuchus ($l = 345°$, $b = 20°$). Since the vast majority of the sources in the original MD excluded zones are in fact Galactic objects of various sorts, we decided to examine all objects in the second and fourth rows in Table 1 on the POSS and ESO Sky Survey red plates, and only observe at the telescope those sources that are resolved to the eye and are thus galaxy candidates. For objects outside the MD excluded zones, all sample objects not clearly associated with Galactic sources were observed at the telescope. The MD excluded zone objects were examined on the sky survey plates by one of us (A. Y.) with the very able assistance of Ludmila Melchior and Karl Fisher. Our philosophy was to reduce the number of objects to be observed at the telescope to a manageable amount, and yet err on the side of caution. There are surely a number of galaxies not observed in the present sample because they are unresolved on the Sky Survey plates; in addition, there are certainly some genuine galaxies that are completely invisible in the optical due to extinction, and are thus invisible on the Sky Survey plates. Of course, even if we knew these latter sources to be galaxies, we would be unable to obtain their optical redshifts in a reasonable amount of time at the telescope. Furthermore, high-redshift *IRAS* galaxies are often powerful nucleated starburst galaxies and can be difficult to differentiate from stars on the sky survey plates. Fisher *et al.* (1990) in fact show evidence that the survey is incomplete at redshifts greater than $\sim 20{,}000$ km s^{-1} and low Galactic latitudes. We have thus begun a program of imaging these low-latitude fields in *R* band, to try to quantify this effect; the results will be reported in future papers. We see little evidence that this is a problem at redshifts below 10,000 km s^{-1}, the limit of our large-scale structure analyses.

There are several ways in which we have quantified our ability to identify galaxies close to the Galactic plane. The first is to check whether the number density of galaxies in the plane region is in agreement, within the limitations of small-number statistics, to that at higher Galactic latitudes. In Table 2, we show the results of this comparison in various of the MD excluded zones, and the Galactic plane divided up into Galactic longitude bins. The expected number of galaxies in each region is just given by the solid angle of the region corrected for the bins affected by confusion, times the mean number density of *IRAS* galaxies on the sky.

Notice the substantial agreement between expected and observed numbers. The effect of superclusters and voids near the Galactic plane is clear in the number counts in the regions close to the plane; the substantial overdensity associated with the Hydra-Centaurus supercluster is particularly prominent ($250° < l < 360°$).

Second, we may compare our results with independent surveys of *IRAS* galaxies close to the plane. In these comparisons, we used an extended sample of objects brighter than 1.2 Jy at 60 μm for which we have made identifications and have started to obtain redshifts. Dow *et al.* (1988) and Lu *et al.* (1990) (see also Kerr and Henning 1987) have used the Arecibo 305 m telescope to search for redshifted 21 cm emission from *IRAS* point sources at Galactic latitudes below $|b| = 16°$; they were sensitive to redshifts less than ~ 9000 km s^{-1}. There are 122 objects in their sample that are also included in ours; they

TABLE 2

STATISTICS IN MEIKSIN AND DAVIS EXCLUDED ZONES

Number Observed	Number Expected	Region
34.....	36	Ophiuchus
12.....	12	Orion
3.....	2	Magellanic Clouds
14.....	13	All others; $\|b\| > 10°$
5.....	19	$5 < \|b\| < 10°$; $0° < l < 36°$
13.....	20	$5 < \|b\| < 10°$; $36° < l < 72°$
14.....	16	$5 < \|b\| < 10°$; $72° < l < 108°$
20.....	19	$5 < \|b\| < 10°$; $108° < l < 144°$
23.....	20	$5 < \|b\| < 10°$; $144° < l < 180°$
18.....	20	$5 < \|b\| < 10°$; $180° < l < 216°$
20.....	20	$5 < \|b\| < 10°$; $216° < l < 252°$
31.....	19	$5 < \|b\| < 10°$; $252° < l < 288°$
34.....	20	$5 < \|b\| < 10°$; $188° < l < 324°$
27.....	18	$5 < \|b\| < 10°$; $324° < l < 360°$

detected redshifted H I emission in 30 of them, of which we identified 28. One of the remaining two objects, I05380+2020, is the lowest signal-to-noise ratio detection in their survey and is identified optically with a Galactic H II region in Lynds (1965). A careful examination of the POSS red plate in the region of the other object that we missed, I05223+1908, did in fact reveal a possible extended object at the limit of detectability. In addition, we identified an additional 18 galaxies with redshifts below 9000 km s^{-1} that they did not detect. Optical identifications thus seem to be more efficient than "blind" radio surveys.

Ichikawa and Nishida (1989) have made optical identifications of *IRAS* point sources in the Ophiuchus star-forming region. Of 37 objects they identified as galaxies, 11 were above 1.2 Jy and thus bright enough to enter our deeper survey in progress; we agreed with their assessment on nine of these objects. Of the remaining two, I16441−2303 is clearly a plate flaw they misidentified as a galaxy, and I16400−2034 is a galaxy that we probably missed because of an oversight.

Kraan-Korteweg (1989) has identified faint galaxies in the low-latitude regions of the Hydra cluster from the ESO sky survey plates. She has compared our list of identifications in the region with hers, and does not find any galaxies that she has identified that we overlooked. There are 31 galaxies in common between our lists. In addition, there are two galaxies that we have identified that she did not include: one low-redshift quasar (Strauss, Kirhakos, and Yahil 1988), and one galaxy of very low surface brightness.

Finally, there is one very low surface brightness, low-redshift MCG galaxy (MCG+07−45−006), discovered by matching the candidate list with the MCG catalog, which was inadvertently identified as infrared cirrus on examination of the Palomar plate. Our conclusion is that we have successfully identified all but a small number of true galaxies among the *IRAS* sources in low-latitude regions, at redshifts less than 10,000 km s^{-1}.

III. ACCURATE FLUX DENSITIES FOR VARIABLE, EXTENDED, AND MODERATE QUALITY SOURCES

Objects within $\approx 5'$ of weeks-confirmed sources in the *IRAS Small Scale Structure Catalog* (1988, hereafter SSC), which consists of sources resolved by the *IRAS* beam, are flagged as extended in the PSC (SES2 flag). As discussed above, the PSC processing involved passing a zero-sum filter with width 2′ at 60 μm over the data stream, and thus systematically underestimates the flux densities of all resolved sources. This may be corrected for, using a procedure known as ADDSCANing. Given the coordinates of the source in question, the individual scans from each detector in a given bandpass that passed within 1.5 of the source position are assembled, and a median scan is derived. Because *IRAS* scanned along lines of near constant ecliptic longitude, all focal plane scans across a given source cross it at approximately the same angle, so this median scan has some physical meaning (see Moshir *et al.* 1989, Fig. II.C.9). For most objects, results using a detector noise-weighted average of the scans give indistinguishable results, but we use the median because it is less sensitive to noise spikes. A quadratic baseline is fitted to the median, and the total flux density between zero crossings of the baseline-subtracted scan is the new estimate of the flux density. The assumption is made that sources are not extended much beyond the $\sim 5'$ length of the slit in the direction perpendicular to the scan; below, we explain how we obtained accurate flux densities for nearby galaxies appreciable larger than this limit. Because we used the zero-crossing flux density, however, we have made no assumptions about the extent of the galaxy *along* the scan direction.

Note how the ADDSCAN procedure differs from that used to estimate the PSC flux densities, as described in § II*a*. The ADDSCAN procedure has three advantages: the use of a median scan increases the signal-to-noise ratio of the detection, it decreases the sensitivity to noise spikes and radiation hits, and because a zero-crossing flux density is used, it includes all the flux density on moderately extended objects.

a) ADDSCANs

With the generous help of Tom Soifer, Elizabeth Smith, Linda Fullmer, and the data management team of the Infrared Processing and Analysis Center (IPAC), we have obtained ADDSCAN flux densities for objects in our survey that fall into one or more of four categories: objects flagged as extended at 60 μm, variable, or of moderate flux quality at 60 μm, or having poor correlation coefficient (CC_{PSC} for PSC correlation coefficient) at 60 μm. Sources are flagged as variable if the flux densities in the 12 and 25 μm bands were seen to vary in the same sense between two sets of hours-confirmed scans (ES, § V.H.5).

Bright sources of moderate flux quality are likely to be either slightly extended, affected by confusion, or affected by noise spikes; ADDSCANing will thus give somewhat more accurate flux densities for these sources.

Finally, there was a handful of sources in the survey, not flagged as variable or extended, for which the CC_{PSC} of the fit of the individual scans to the PSC template was less than 99%; presumably these sources are of low signal-to-noise ratio and were also included for ADDSCANing. We did *not* include sources with $f_{60} < 1.936$ Jy with poor CC_{PSC} in the sample. There are 1355 such objects not flagged as extended or variable; inspection of the POSS and ESO Sky Survey prints of a sample of these showed the vast majority to be associated with infrared cirrus. So although ADDSCANing would undoubtedly bring some number of these objects above our flux density limit, we decided not to include them in the present sample. Further aspects of the poor CC_{PSC} problem are discussed at the end of this section.

The flux densities from the ADDSCAN procedure were corrected for a small calibration error empirically derived by Gene Kopan (private communication), to bring them in line with the PSC flux scale; this correction amounts to −6.6% at 60 μm. This calibration error was corrected in the ADDSCAN procedure in 1989 March, and thus the last set of objects ADDSCANed, the sources of moderate flux quality, did not have this correction applied.

A total of 3585 objects in Table 1 were ADDSCANed, of which 710 are galaxies with corrected flux densities above 1.936 Jy, and 12 are as yet unobserved. We had already rejected a number of the faint extended and variable objects as Galactic objects before the ADDSCANing was done, so the ADDSCAN data are complete only for the confirmed galaxies. In addition, there are five galaxies flagged as extended, with PSC fluxes above 1.936 Jy, for which we did not obtain ADDSCANs because of a bookkeeping error. They are included in rows 1 and 2 of the table.

Unfortunately, there are at least two effects that can give ADDSCAN flux densities in error. A source might be flagged as extended if it consists of a pair of galaxies not cleanly

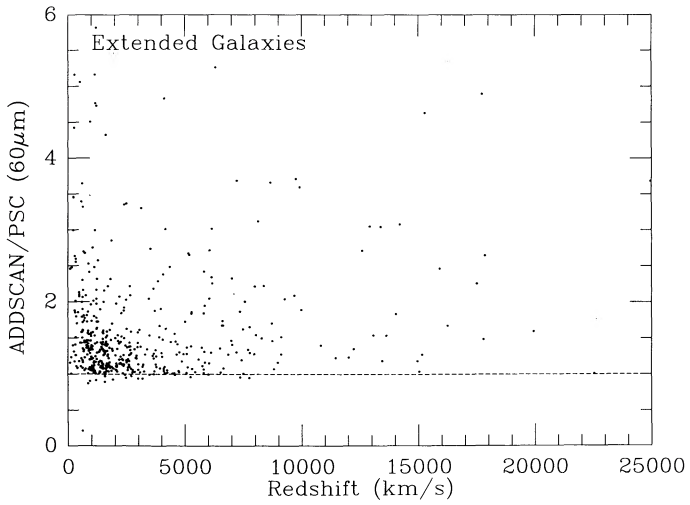

FIG. 7.—The ratio of ADDSCAN to PSC 60 μm flux densities vs. redshift for all galaxies flagged as extended in the sample.

separated at the resolution of the *IRAS* beam (see Moshir *et al.* 1989, Fig. III.D.1). Clearly, this will be a more important effect at larger distances than small. It is not clear how to correct for this in analyses of large-scale structure. Should the two objects be counted as one? Perhaps each alone is luminous enough to make the flux density limit, and the pair should be counted as two; after all, interacting galaxies are known to have enhanced far-infrared emission (e.g., Bushouse *et al.* 1988). Alternatively, because most of these sources will have a *total* flux density only slightly larger than the flux limit, it is likely that neither galaxy alone belongs in the catalog, and so the source should be tossed out altogether. There are similar problems in existing optical catalogs; $\sim 10\%$ of the objects at 15th magnitude in the Zwicky (1961–1968) catalog of galaxies are doubles that Zwicky counted as one (J. Huchra, private communication). A further difficulty is shown by extreme examples of interacting systems; the extremely luminous *IRAS* galaxy Mrk 231 has recently been shown to have extended tails suggestive of a merger event (e.g., Sanders *et al.* 1988), but no one would consider calling this object a pair of galaxies. With these ambiguities in mind, we will consider unresolved doubles as a single source.

Second, galaxies might be confused with Galactic sources in the foreground. There are a number of galaxies flagged as extended at 12 μm lying within 1′ of a bright foreground star. Even more common are distant galaxies which lie in a haze of foreground cirrus, which can cause the SES2 flag to be raised at 60 μm. Perhaps in the latter case, the PSC flux density is a more reliable estimator of the true flux density from these objects.

We tested for these systematic effects as follows. Figure 7 is a scatterplot of the ratio of the ADDSCAN to PSC flux density ratio at 60 μm, as a function of redshift, for the galaxies flagged as extended. Note that there is *not* a strong decrease in the average ADDSCAN to PSC ratio as the redshift increases. There are 128 sources in our sample, flagged as extended, but with redshifts greater than 5000 km s^{-1}, which are thus unlikely to be resolved by the *IRAS* beam. The finding charts for these objects were mixed with a random selection of galaxies with the same redshift range, but not flagged as extended. In only a few cases did the SES2 objects stand out on the finding charts with an obvious reason to be flagged as extended. We conclude that we are probably not contaminating our sample unduly with such sources. In a future paper, we show that the substitution of PSC flux densities for ADDSCAN flux densities for these 128 sources has a miniscule effect on the large-scale structure analyses.

A further test is shown in Figure 8, which shows the sky distribution of these 128 objects. To our great relief, they do not shown any strong concentration to the Galactic plane. There is, however, a surfeit of objects at the north ($l = 96°$, $b = +30°$) and south ($l = 276°$, $b = -30°$) ecliptic poles. Because of the geometry of the *IRAS* survey, sources near the poles were scanned a great number of times. Thus the probability of noise or foreground emission bringing a source into the SSC is enhanced in this region.

In Figure 9, we show the ratio of ADDSCAN to PSC flux densities at 60 μm for all the objects for which we obtained ADDSCANs, as a function of the CC_{ADD} of the point source template to the ADDSCAN median scan, a sort of goodness of fit. Note that the PSC and ADDSCAN correlation coefficients are derived in different ways and need not be equal. As might

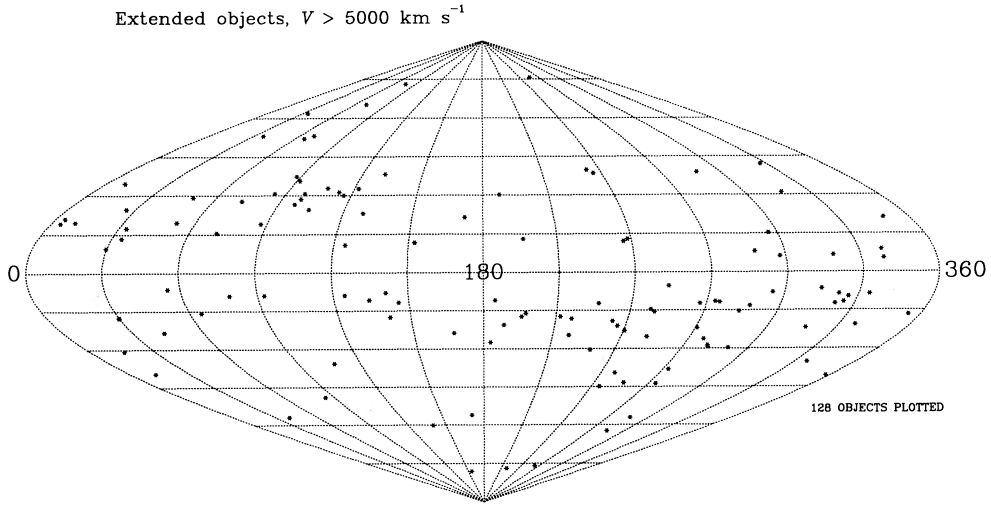

FIG. 8.—The sky distribution of all galaxies flagged as extended with redshifts greater than 5000 km s^{-1}

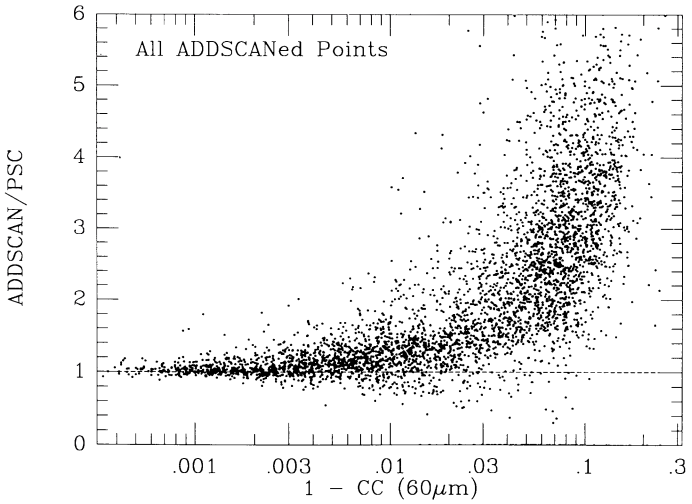

FIG. 9.—The ratio of ADDSCAN to PSC 60 μm flux densities as a function of $1 - CC_{ADD}$ for the 4309 objects for which we obtained ADDSCANs. Note that this is a larger number than is listed in Table 1; many of these objects did not get included in the final sample.

be expected, there is a strong anticorrelation between these two quantities. It was disturbing, however, that sources with CC_{ADD} as large as 0.999 still show appreciably larger ADDSCAN than PSC flux density.[6] In the PSC, the CC_{PSC} is listed: it is the *best* correlation coefficient from all the individual scans crossing the source, and it is only listed to an accuracy of two decimal places. In order to check that there was not a vast population of galaxies with one good scan and many scans with poor correlation coefficient not indicated in the PSC, we matched all of our galaxies not flagged as extended, variable, or of moderate flux quality at 60 μm, against the Working Survey Data Base, which lists CC for all individual scans. Two hundred fifty-seven of the 1755 such sources had less than perfect CC. These are presumably due to excess noise entering one or more of the scans. In Fig. 10, we show the ratio of ADDSCAN to PSC flux densities at 60 μm as a function of

[6] Note, however, that the ADDSCAN CC is based on an *oversampled* median scan, and so is not directly comparable to the PSC CC.

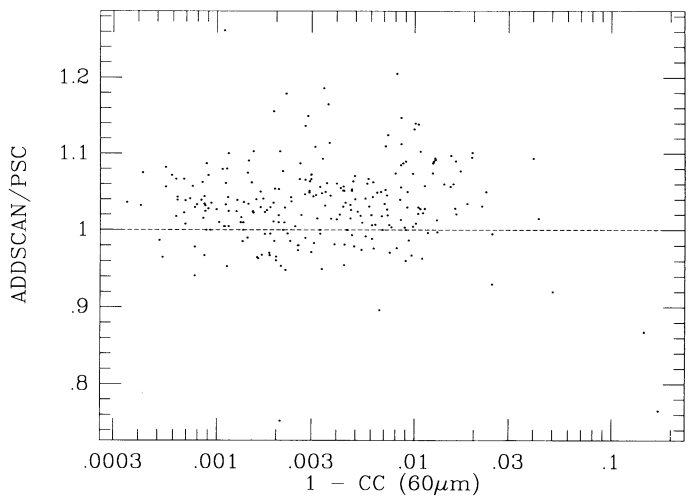

FIG. 10.—As in Fig. 9, for those objects in our survey with poor CC in at least one entry in the Working Survey Data Base.

CC_{ADD} for these sources. Because we have no reason to believe these galaxies are extended, we have used the amplitude of the PSC template fit to the median scan, rather than the zero-crossing flux density. The result is reassuring: almost no sources have their flux densities changed by more than 20%. Thus we use the PSC flux density, rather than the ADDSCAN flux density, for these sources.

Figures 11*a*–11*c* show subsets of the data in Figure 9, for galaxies flagged as extended, variable, and of moderate flux quality, respectively. There is an appreciable number of sources that fall into two or all three of these categories; they are plotted in all relevant figures. It is reassuring that the majority of the objects with poor CC_{ADD} and concomitant large ADDSCAN to PSC ratio in Figure 9 are not galaxies. Note that the variable and moderate flux quality galaxies tend to have high CC_{ADD}, and thus relatively small corrections to their flux densities, while many of the extended sources have much larger corrections.

b) Galaxies of Large Angular Size

As mentioned above, the ADDSCAN procedure cannot derive accurate flux densities for sources with angular extents greater than $\sim 5'$. Rice *et al.* (1988, hereafter LOGC for Large Optical Galaxy Catalog) have derived accurate flux densities for all objects in the *Second Reference Catalogue of Galaxies* (de Vaucouleurs, de Vaucouleurs, and Corwin 1976) with angular diameters greater than 8′; we have incorporated into our sample those flux densities derived from the two-dimensional co-adding procedure. This adds 13 galaxies to our sample, most of which are in the Local Group, and updates the flux densities of 46 more. Figure 12 shows the comparison of PSC and LOGC flux densities for these objects. Note that the LOGC is not complete; Table 8 of Rice *et al.* (1988) lists 55 galaxies with *corrected* diameters above the 8′ limit of the LOGC, but not included in the sample. We use ADDSCAN flux densities for these objects.

Finally, we worried about galaxies of intermediate angular size ($3' \lesssim \theta < 8'$) which did not appear in the PSC. The SSC consists of 16,740 objects detected as point sources in the *IRAS* data base when running zero-sum filters of size 2′, 4′, and 8′ were convolved with the *IRAS* data stream. Of these objects, 2073 fit our selection criteria above, and are not already in the PSC. The vast majority of these are at low Galactic latitudes, and trace out the MD excluded zones. Only 16 have been identified with galaxies in existing optical catalogs; 14 of these are galaxies of small angular size seen behind a haze of foreground cirrus, and two are already included in the LOGC. Because the SSC is known to be incomplete below ~ 5 Jy at 60 μm, we decided not to include any additional objects from the SSC in our sample.

c) A Test

After all this work, can we get any sense of how good our flux densities are? Valenti and Filippenko (1990) have compiled accurate *IRAS* flux densities in all four bands for the 500 brightest optical galaxies in the northern hemisphere. Their flux densities are based on ADDSCANs, using the weighted mean scans rather than the median scan; unlike us, they have gone to considerable trouble to exclude individual scans contaminated by noise spikes and radiation hits. There are 46 galaxies in our sample for which Valenti and Filippenko rejected at least one scan at 60 μm because of contamination. Figure 13 is a scatterplot of their and our flux densities at 60 μm.

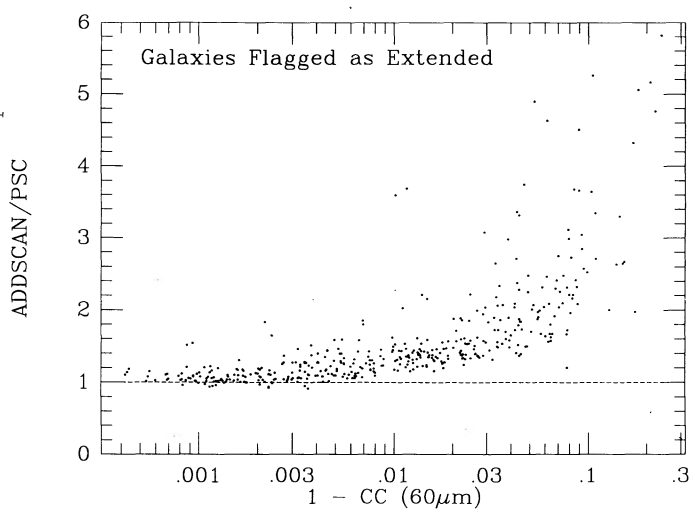

FIG. 11*a*

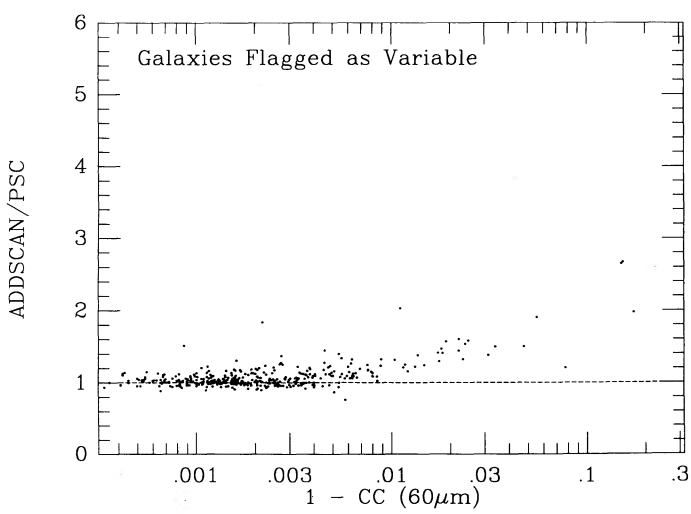

FIG. 11*b*

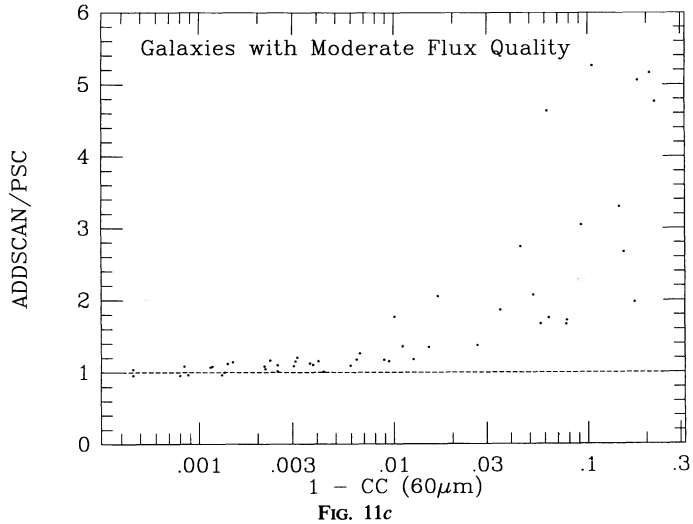

FIG. 11*c*

FIG. 11.—(*a*) As in Fig. 9, for the 439 galaxies in the sample flagged as extended at 60 μm. (*b*) As in Fig. 9, for the 395 galaxies in the sample flagged as variable. (*c*) As in Fig. 9, for the 57 galaxies in the sample of moderate flux quality at 60 μm. Note that the samples depicted in (*a*)–(*c*) are *not* mutually exclusive.

Almost all the sources are in excellent agreement. Of the 10 sources for which we disagree by more than 10%, three are in the LOGC, which has more accurate flux densities than those derived by ADDSCANing. Valenti and Filippenko use a number of estimators of flux density involving various weightings for the different scans. For most of their objects, the different estimators give consistent results; the rest of the sources in large disagreement in Figure 13 are objects in which the various Valenti and Filippenko flux density estimators are *not* in agreement among themselves.

Soifer *et al.* (1989) have compiled ADDSCAN flux densities for their sample of bright northern *IRAS* galaxies, using similar procedures to ours. Of the 305 galaxies in common in the two samples, nine differ in 60 μm flux density by more than 20%. We use LOGC fluxes for six of these, which we believe are superior to ADDSCAN fluxes; the remaining three are all galaxies with close companions, and thus are affected by confusion.

IV. HYSTERESIS CORRECTION

As emphasized above, our principal aim is to eliminate all systematic biases in the flux scale that could mimic large-scale inhomogeneities in the sample. One such effect is due to hysteresis. When the *IRAS* detectors passed over regions of high flux density, their responsivity was momentarily increased (ES, § IV.A.8). This is corrected for to some extent by internal calibrations done at the end of each scan at the ecliptic poles, but see ES, § VI.B.4.*c* for the description of the limitations of this technique to correct for hysteresis. At 100 μm, a further statistical correction for hysteresis was performed (ES, § VI.B.4.*c*); we will use the same technique to correct at 60 μm. See Deul and Walker (1989) for a related approach to this problem.

The principal sources of hysteresis in the sky are extremely bright objects on small scales and, on larger scales, the South Atlantic Anomaly and the Galactic plane. As the South Atlantic Anomaly is fixed on the Earth, it does not effect any one area of the sky and is thus unlikely to cause serious systematic effects. With the help of Tim Conrow of IPAC, we measured

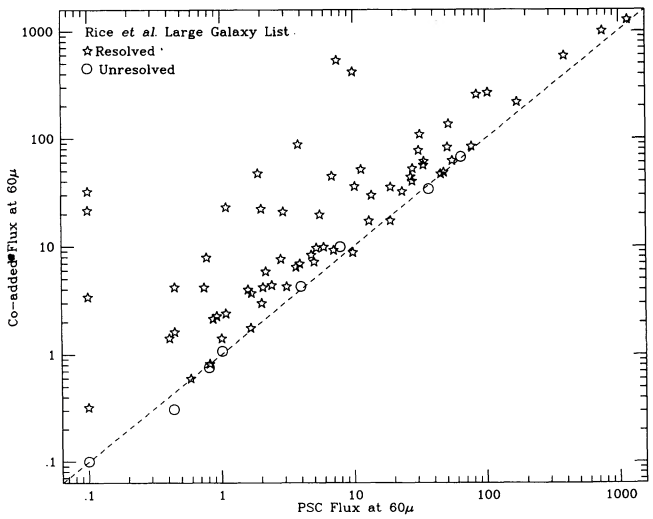

FIG. 12.—Scatterplot of 60 μm flux densities in the LOGC vs. those in the PSC for the galaxies in common in the sample. Sources extended in the *IRAS* data are indicated by stars, while those unresolved are indicated by circles. We have adopted PSC fluxes for the latter sources. The line is $x = y$.

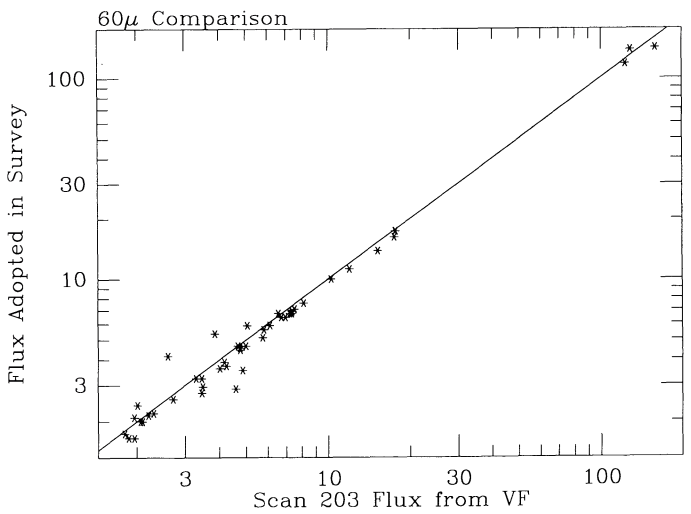

FIG. 13.—Scatterplot of 60 μm flux densities in the Valenti and Filippenko (1990) sample vs. those in our sample for the galaxies in both samples which have at least one scan rejected in the Valenti and Filippenko analysis. The line is $x = y$.

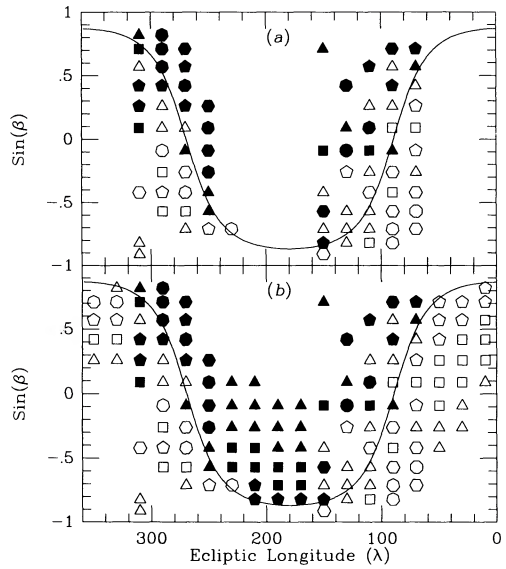

FIG. 14.—(*a*) Ratio r of the flux density derived from ascending and descending scans, respectively, as a function of ecliptic coordinates λ and β. Only those bins with 20 or more objects are shown. Open symbols indicate bins with $r < 1$, while solid symbols are for sources with $r > 1$. The number of sides of the symbol is given by $100 \times |r - 1| + 3$. The Galactic plane is indicated by the solid line. (*b*) The results of the previous plot extrapolated to the full length of the Galactic plane.

the hysteresis effects from the Galactic plane as follows: we selected a sample of 7032 point sources, "clean" at 60 μm; that is, not flagged as extended or variable, and with highest flux quality. Because *IRAS* scanned along lines of constant ecliptic longitude, the scan lines crossed the Galactic plane at approximately right angles, so that individual scans crossing a given source may be divided into ascending and descending with respect to the Galactic plane. A scan crossing the plane *before* crossing a given source will be subject to hysteresis and thus will be expected to have systematically larger flux density than a scan going the other way. Thus, for each of these sources, we compiled the ratio of the average of flux densities derived on the ascending and descending scans, respectively. This analysis was, of course, only possible in those areas of the sky in which the survey strategy had been such as to include at least one scan in each direction. The average ascending to descending flux density ratio, r, in bins 20° in ecliptic longitude by 10° in ecliptic latitude is shown in Figure 14*a*. Only those bins with 20 or more objects are shown. Open symbols indicate bins with $r < 1$, while solid symbols are for sources with $r > 1$. The number of sides of the symbol is given by $100 \times |r - 1| + 3$, thus a solid pentagon represents a value of $r = 1.02$. As we might expect, r changes sign when crossing the Galactic plane, and the effect is strongest closest to the plane, and near the Galactic center. Following the similar analysis in ES, § VI.B.4.*c*, we extrapolated this hysteresis pattern to regions of the sky not covered by ascending and descending scans; this is shown in Figure 14*b*. Within 30° of the ecliptic poles, there are scans in so many directions that hysteresis effects will average out.

In order to calculate a correction to a flux density of a source at a given spot, we need to know the relative number of ascending and descending scans. At low ecliptic latitudes, this is simply a function of ecliptic longitude, given in Table 3. We presume that the correct flux density is given by equal numbers of ascending and descending scans (as was done at 100 μm), and we thus can derive fractional corrections for hysteresis, for any source in the sky, given its position. In Figure 15, we show the resulting corrections for the galaxies in our sample as a function of galactic longitude. There is a striking quadrupole moment, but almost no flux densities are corrected by more than 1%, and none more than 2.2%. Although there are a few objects in the PSC whose flux densities are changed by this correction enough to affect their inclusion in the catalog, none of these are galaxies, and thus we do *not* apply the correction to our sample.

Note that the responsivity enhancement close to the plane has a steep gradient, and the large bin size we used may dilute the hysteresis effect (W. Rice, private communication). Thus we may be underestimating the size of the correction close to the Galactic plane. In addition, there may be hysteresis effects at 12 and 25 μm as well, which could effect our color criterion. This is unlikely to be a serious problem, as few galaxies are found near the color limit line in Figure 3.

V. DISCUSSION AND SUMMARY

Our final catalog, then, consists of 5014 sources satisfying our criteria. Of these, 2649 are confirmed galaxies with redshifts; their sky distribution is shown in Figure 16 (cf. Fig. 5 for the excluded zones), and 13 have not been observed at this time. The remainder are identified with cirrus, molecular

TABLE 3

NUMBER OF ASCENDING AND DESCENDING SCANS

Ecliptic λ Range	Number Ascending	Number Descending
$35° < \lambda < 59°$	3	0
$59° < \lambda < 157°$	1	2
$157° < \lambda < 212°$	0	2
$212° < \lambda < 239°$	0	3
$239° < \lambda < 327°$	2	1
$327° < \lambda < 35°$	2	0

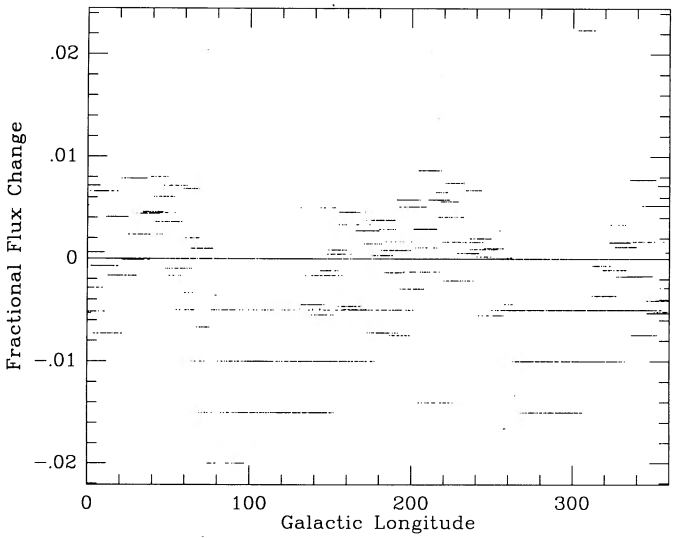

FIG. 15.—The hysteresis correction as a function of Galactic longitude. Nowhere is it more than 2.2%.

clouds (with imbedded sources inside?), emission-line, and T Tauri stars, planetary nebulae, and H II regions in both our Galaxy and other resolved galaxies. Their sky distribution is shown in Figure 17. Finally, Figure 18 shows the sky distribution of the remaining objects without redshifts.

There are a few outstanding issues remaining in the sample selection. As mentioned above, we are in the process of extending our survey to 1.2 Jy at 60 μm; we hope to address these problems in this deeper sample as well. The first such problem is the difficulty of distinguishing high-redshift galaxies from stars at low Galactic latitudes. We have seen evidence that our sample is incomplete at redshifts above $\sim$20,000 km s^{-1} at low Galactic latitudes (Fisher *et al.* 1990) and have started a program of optical imaging of many low-latitude fields to try to quantify (and if possible, to correct) this effect.

We are also worried about the nature of the high-redshift extended objects and would like to understand what it is that triggers the extended flag in the PSC for these sources. We intend to obtain two-dimensional co-additions of the *IRAS* data in these fields, and compare them with the optical images,

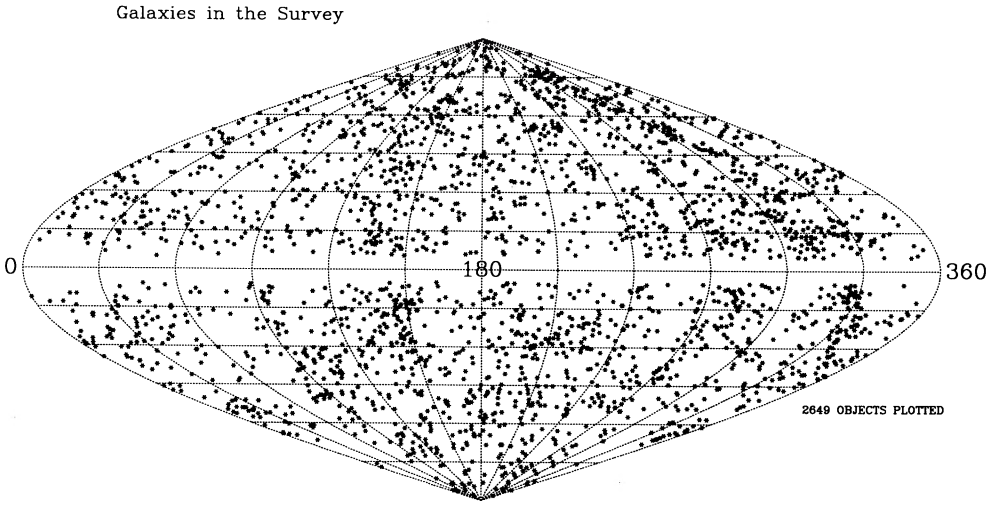

FIG. 16.—The sky distribution of galaxies in the sample

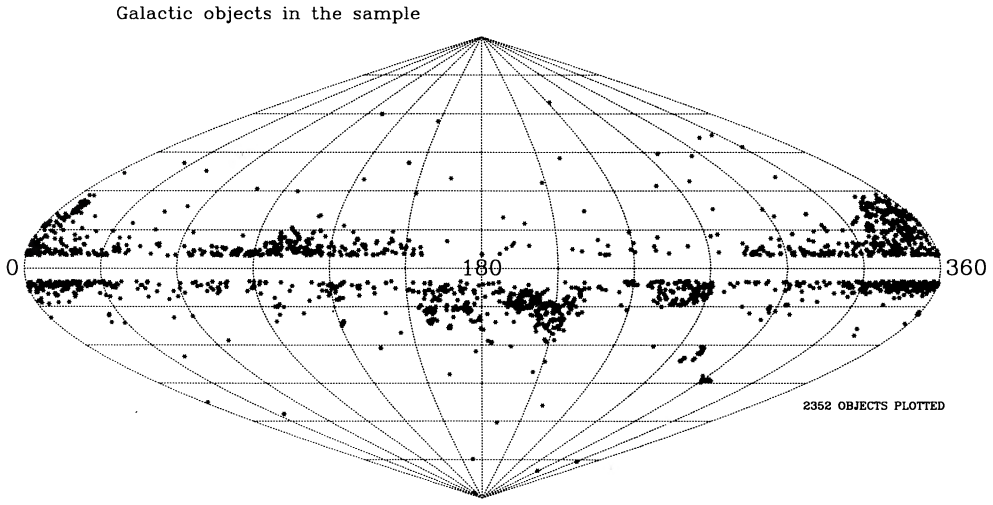

FIG. 17.—The sky distribution of Galactic objects in the sample

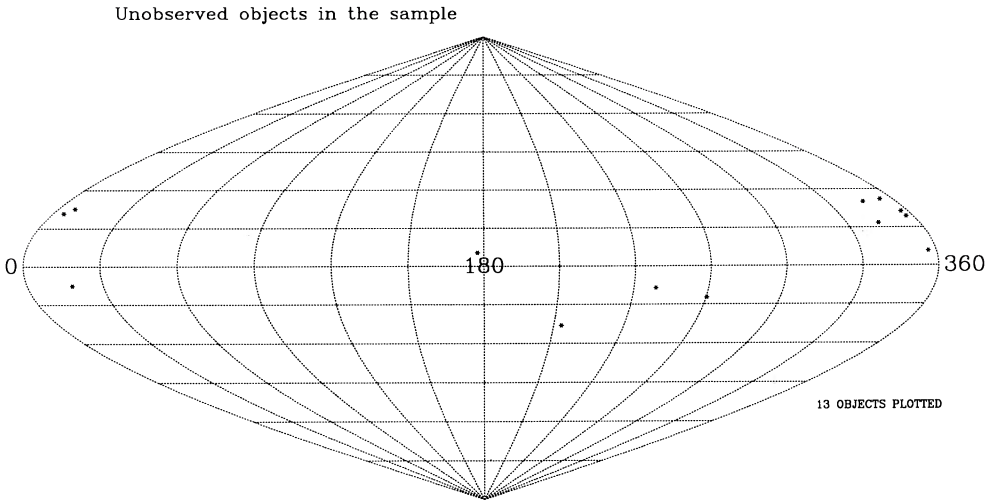

FIG. 18.—The sky distribution of unobserved objects in the sample. Note that they are concentrated in the Orion and Ophiuchus regions.

to look for extended structure caused by neighboring objects or foreground cirrus.

C. Lonsdale (private communication) points out that sources that are slightly resolved at 60 μm (i.e., with optical diameters between 2′ and 3′) may not trigger the SES2 flag, and will thus have fluxes underestimated by typically 20%–30%. Similarly, sources with diameters between 5′ and 8′ may have ADDSCAN fluxes that are underestimates, since they are larger than the slit length. A closer look at the median scans produced by the ADDSCAN procedure promises to identify sources affected by these problems.

Finally, we have not really demonstrated that the ADDSCAN procedure gives identical results to the PSC procedure in the limit of unresolved, high signal-to-noise ratio sources. We have recently obtained ADDSCANs of a large number of "clean" *IRAS* galaxies to address these questions.

The results of these investigations will be reported when we complete the 1.2 Jy survey.

This paper may be summarized as follows: We have used the *IRAS* data base to select a sample of 5014 objects satisfying the following criteria:

1. $f_{60}^2 > f_{12} f_{25}$, based on flux densities or upper limits listed in the PSC;
2. Flux quality at 60 μm moderate or high;
3. $f_{60} > 1.936$ Jy.

The sample includes 2649 galaxies; 13 further objects are not yet observed. The sample covers 87.6% of the sky. Objects within 5° of the Galactic plane, in regions limited by confusion at 60 μm, or of incomplete coverage by the *IRAS* survey are not included. We obtained accurate flux densities for objects flagged as extended at 60 μm, variable, or of moderate flux quality, using the ADDSCAN procedure. Hysteresis due to enhanced responsivity of the *IRAS* detectors upon crossing the Galactic plane is measured and found to be less than a 2% effect.

In future papers in this series, this sample will be used to study the large-scale distribution of galaxies and the resulting inferred velocity field.

In a project of this size, there are a very large number of people to thank. First, the entire IPAC staff has been extremely helpful in answering our numerous questions about the *IRAS* data processing procedures and cheerfully handling our requests for literally thousands of ADDSCANs; we especially want to thank Tom Soifer, Tom Chester, Elizabeth Smith, Linda Fullmer, Walter Rice, Carol Lonsdale, George Helou, and Gene Kopan. Tim Conrow went out of his way to prepare the material needed for the analysis of hysteresis in § IV. We thank the National Space Science Data Center at the NASA–Goddard Space Flight Center for providing us with tapes of the *IRAS* PSC Version 2 and the CGIRAS. We have benefited greatly from many discussions about the *IRAS* and optical data processing with Avery Meiksin, Pat McCarthy, Kate Ebneter, and Simon White. Ludmila Melchior is thanked for her assistance in examining several thousand *IRAS* sources close to the plane. Karl Fisher assisted in the analysis of high-redshift extended objects (§ III*a*), and he and Arjun Dey worked on the analysis of the color criterion. Renée Kraan-Korteweg supplied us with her optical identifications of galaxies in the Hydra region before publication, and we had interesting discussions with Nanyao Lu about the Arecibo observations. Jeff Valenti supplied a machine-readable version of his results before publication and was a great source of information on ADDSCANs. Rosie Wyse and Dave Burstein made many useful comments on the text, and the suggestions of Walter Rice's referee report clarified many points. This research has been supported in part under the *IRAS* extended mission program and by a grant from the NSF. J. P. H. has been partially supported by NASA grant NAGW-201. M. A. S. acknowledges the support of a National Science Foundation Graduate Fellowship and a Berkeley Graduate Fellowship.

REFERENCES

Babul, A., and Postman, M. 1990, *Ap. J.*, **359**, 280.
Bahcall, N. A., and Soneira, R. M. 1983, *Ap. J.*, **270**, 20.
Bothun, G. D., Lonsdale, C. J., and Rice, W. 1989, *Ap. J.*, **341**, 129.
Brown, M. E., and Groth, E. J. 1989, *Ap. J.*, **338**, 605.
Bushouse, H. A., Lamb, S. A., and Werner, M. W. 1988, *Ap. J.*, **335**, 74.
Cataloged Galaxies and Quasars Observed in the IRAS Survey, Version 2. 1989, prepared by C. J. Lonsdale, G. Helou, J. C. Good, and W. L. Rice (Pasadena: Jet Propulsion Laboratory) (CGIRAS).
Cohen, M., Schwartz, D. E., Chokshi, A., and Walker, R. G. 1987, *A.J.*, **93**, 1199.

Crawford, J., and Rowan-Robinson, M. 1986, *M.N.R.A.S.*, **221**, 53.
de Lapparent, V., Kurtz, M. J., and Geller, M. J. 1986, *Ap. J.*, **304**, 585.
de Vaucouleurs, G., de Vaucouleurs, A., and Corwin, H. G., Jr. 1976, *Second Reference Catalogue of Bright Galaxies* (Austin: University of Texas Press).
Dekel, A., Blumenthal, G. R., Primack, J. R., and Olivier, S. 1989, *Ap. J. (Letters)*, **338**, L5.
Deul, E. R., and Walker, H. J. 1989, *Astr. Ap. Suppl.*, **81**, 207.
Dey, A., Strauss, M. A., and Huchra, J. 1990, *A.J.*, **99**, 463.
Dow, M. W., Lu, N. Y., Houck, J. R., Salpeter, E. E., and Lewis, B. M. 1988, *Ap. J. (Letters)*, **324**, L51.
Fisher, K., Strauss, M. A., Davis, M., Yahil, A., and Huchra, J. P. 1990, *Ap. J.*, submitted.
Geller, M. J., de Lapparent, V., and Kurtz, M. J. 1984, *Ap. J. (Letters)*, **287**, L55.
Groth, E. J., and Peebles, P. J. E. 1986*a*, *Ap. J.*, **310**, 499.
———. 1986*b*, *Ap. J.*, **310**, 507.
Hacking, P. B., Condon, J. J., and Houck, J. R. 1987, *Ap. J. (Letters)*, **316**, L15.
Heisler, C., and Vader, P. 1989, in *IAU Symposium 134, Active Galactic Nuclei*, ed. D. E. Osterbrock and J. S. Miller (Dordrecht: Kluwer), p. 408.
Helou, G. 1986, *Ap. J. (Letters)*, **311**, L33.
Hughes, V. A., and MacLeod, G. C. 1989, *A.J.*, **97**, 786.
Ichikawa, J., and Nishida, M. 1989, *A.J.*, **97**, 1074.
IRAS Catalogs and Atlases, Explanatory Supplement. 1988, ed. C. A. Beichman, G. Neugebauer, H. J. Habing, P. E. Clegg, and T. J. Chester (Washington, DC: US Government Printing Office) (ES).
IRAS Point Source Catalog, Version 2. 1988, Joint *IRAS* Science Working Group (Washington, DC: US Government Printing Office) (PSC).
IRAS Small Scale Structure Catalog. 1988, prepared by G. Helou and D. W. Walker (Washington, DC: US Government Printing Office) (SSC).
Kerr, F. J., and Henning, P. A. 1987, *Ap. J. (Letters)*, **320**, L99.
Kraan-Korteweg, R. C. 1989, in *ASP Conf. Series, Large Scale Structures and Peculiar Motions in the Universe*, ed. D. Latham and N. L. da Costa (San Francisco: ASP), in press.
Low, F. J., *et al.* 1984, *Ap. J. (Letters)*, **278**, L19.
Low, F. J., Huchra, J. P., Kleinmann, S. G., and Cutri, R. M. 1988, *Ap. J. (Letters)*, **327**, L41.
Lu, N. Y., Dow, M. W., Houck, J. R., Salpeter, E. E., and Lewis, B. M. 1990, *Ap. J.*, in press.
Lynds, B. T. 1965, *Ap. J. Suppl.*, **12**, 163.
Meiksin, A., and Davis, M. 1986, *A.J.*, **91**, 191 (MD).
Meurs, E. J. A., and Harmon, R. T. 1988, *Astr. Ap.*, **206**, 53.
Moshir, M., *et al.* 1989, *Explanatory Supplement to the IRAS Faint Source Survey, Version 1* (Pasadena: Jet Propulsion Laboratory).
Neugebauer, G., *et al.* 1984, *Ap. J. (Letters)*, **278**, L1.
Puget, J.-L. 1988, in *Comets to Cosmology*, ed. A. Lawrence (Berlin: Springer), p. 113.
Rice, W. L., Lonsdale, C. J., Soifer, B. T., Neugebauer, G., Kopan, E. L., Lloyd, L. A., de Jong, T., and Habing, H. J. 1988, *Ap. J. Suppl.*, **68**, 91 (LOGC).
Rowan-Robinson, M. 1988, in *Comets to Cosmology*, ed. A. Lawrence (Berlin: Springer), p. 348.
Sanders, D. B., Soifer, B. T., Elias, J. H., Madore, B. F., Matthews, K., Neugebauer, G., and Scoville, N. Z. 1988, *Ap. J.*, **325**, 74.
Saunders, W., Rowan-Robinson, M., Lawrence, A., Efstathiou, G., Kaiser, N., Ellis, R. S., and Frenk, C. S. 1990, *M.N.R.A.S.*, **242**, 318.
Schmidt, M. 1968, *Ap. J.*, **151**, 393.
Shane, C. D., and Wirtanen, C. A. 1967, *Pub. Lick Obs.*, **22**, Part I.
Soifer, B. T., Boehmer, L., Neugebauer, G., and Sanders, D. B. 1989, *A.J.*, **98**, 766.
Soifer, B. T., Houck, J. R., and Neugebauer, G. 1987, *Ann. Rev. Astr. Ap.*, **25**, 187.
Soifer, B. T., Sanders, D. B., Madore, B. F., Neugebauer, G., Danielson, G. E., Elias, J. H., Lonsdale, C. J., and Rice, W. L. 1987, *Ap. J.*, **320**, 238.
Strauss, M. A. 1989, Ph.D. thesis, University of California, Berkeley.
Strauss, M. A., Kirhakos, S. D., and Yahil, A. 1988, *Ap. J. (Letters)*, **332**, L45.
Sutherland, W. 1988, *M.N.R.A.S.*, **234**, 159.
Valenti, J., and Filippenko, A. V. 1990, in preparation.
Walker, H. J., Cohen, M., Volk, K., Wainscoat, R. J., and Schwartz, D. E. 1989, *A.J.*, **98**, 2163.
Yahil, A., Walker, D., and Rowan-Robinson, M. 1986, *Ap. J. (Letters)*, **301**, L1 (YWR).
Zwicky, F., *et al.* 1961–1968, *Catalog of Galaxies and Clusters of Galaxies* (Pasadena: California Institute of Technology).

MARC DAVIS: Astronomy Department, University of California, Berkeley, CA 94720
internet: marc@bkyast.berkeley.edu

JOHN P. HUCHRA: Center for Astrophysics, 60 Garden Street, Cambridge, MA 02138
internet: huchra@cfa3.harvard.edu

MICHAEL A. STRAUSS: Astronomy Department, MS 105-24, California Institute of Technology, Pasadena, CA 91125
internet: mas@deimos.caltech.edu

AMOS YAHIL: Astronomy Program, State University of New York, ESS Building, Stony Brook, NY 11794–2100
internet: ayahil@sbast4.sunysb.edu